Gas transfer model to design a ventilator for neonatal total liquid ventilation

Mirko Bonfanti [a], Antonio Cammi [b], Paola Bagnoli [a,*]

[a] *Laboratory of Biological Structure Mechanics, Department of Chemistry, Materials and Chemical Engineering "Giulio Natta", Politecnico di Milano, Piazza Leonardo da Vinci 32, 20133 Milan, Italy*
[b] *Department of Energy, Nuclear Engineering Division (CeSNEF), Politecnico di Milano, Via Lambruschini 4, 20156 Milan, Italy*

Received 30 November 2014
Revised 12 June 2015
Accepted 11 September 2015

1. Introduction

The evaluation of gas transfer phenomena by numerical modeling is fundamental to design and optimize the performance of respiratory support devices [1,2]. This is particularly important when designing a ventilator prototype for neonatal Total Liquid Ventilation (TLV), since with this technique the fluid dynamics and gas transfer in the lungs and in the ventilator are completely different from conventional gas ventilation (GV), due to the use of liquid perfluorocarbons (PFC) to drive respiratory gases into the lungs [3,4].

TLV is studied as an alternative technique to GV for the treatment of pulmonary pathologies characterized by the lack or absence of endogenous surfactant (e.g. Neonatal Respiratory Distress Syndrome) that affect very low birth weight neonates (i.e. neonates with body weight at birth lower than 1 kg or gestational age lower than 28 weeks) [5,6]. Experimental animal studies proved that TLV is able to support pulmonary gas exchange while preserving lung structures and functions [7]. Moreover, liquid PFC is an optimal ventilation medium due to high oxygen (O_2) and carbon dioxide (CO_2) solubility and suitable chemical properties (i.e. low surface tension, high density, biocompatibility) [5,6]. However, different aspects of TLV have to be improved for a safe transition from the laboratory experience to the clinical application. A key role is played by the development of an advanced device able to safely support gas exchanges, while avoiding lung injury.

Several international research groups proposed various prototypes [8–12], all aimed to perform ventilation and PFC reconditioning (oxygenation, CO_2 removal, and temperature control). The most common strategy is the volume-controlled ventilation. However, to be safe, the volume control devices should be pressure limited, because high inspiratory pressure may induce barotrauma and excessive negative expiratory pressure, due to active PFC drainage, may cause airways collapse [13–15]. Despite these precautions, a number of drawbacks related to tidal volume regulation, gas exchange efficiency and control of the airway pressure are still affecting the outcomes of the trials with volumetric devices. To overcome these limitations, during the Round Table discussion at the "6th International Symposium on Perfluorocarbon Application and Liquid Ventilation" [16], the international scientific community working in TLV field has joined the efforts to define the main specifications TLV treatment has to comply with in terms of devices and controls to be implemented

* Corresponding author. Tel.: + 39 02 23994308; fax: +39 02 23994286.
E-mail address: paola.bagnoli@polimi.it (P. Bagnoli).
URL: http://www.labsmech.polimi.it (P. Bagnoli)

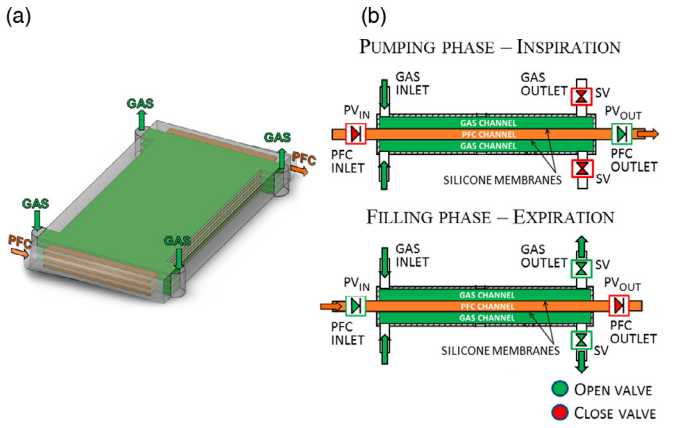

Fig. 1. Schematic configuration of the ventilator prototype: (a) 3D rendering of the Pro-Li-Ve, the arrows highlight the PFC (orange) and gas (green) inlets and outlets; (b) representation of a single Pro-Li-Ve functional module during the pumping (up) and filling (bottom) phases (PV_{IN}: PFC inlet passive valve, PV_{OUT}: PFC outlet passive valve, SV: gas outlet solenoid valve).

to guarantee the safety of the treatment. In this context, Robert et al. (2010) [17] proposed a new controller of their volumetric TLV ventilator [11] able to perform the expiration in pressure controlled strategy [17].

In compliance with the guidelines defined during the Round Table [16], our research group is investigating an alternative approach to develop an innovative Liquid Ventilator Prototype (Pro-Li-Ve) for the treatment of very preterm neonates, able to perform TLV in a lung-protective strategy. This device integrates the pumping and oxygenation functions in a non-volumetric pulsatile device, able to adjust the pumped PFC flow rate depending on the afterload (i.e. lung impedance) [18–20].

The device geometry and fluid dynamics have to be optimized to obtain the desired gas exchange performance, in particular to improve CO_2 removal, which is the main limiting issue in this kind of devices, due to the low partial pressure difference between the 2 compartments [21]. A computational approach is a useful tool for the design process, allowing the optimization of the device prior to construct the prototypes.

The aim of this study was to implement a two-dimensional (2D) semi-empirical computational model to study O_2 and CO_2 exchange between the PFC and the oxygenating gas mixture, as a function of the parameters of the device. The effect on gas exchange exerted by different geometries and ventilation parameters was analyzed to define the best device configuration, able to guarantee the desired gas transfer.

2. Materials and methods

The design of the new prototype consists in a modular device comprising several functional modules, each made of two flat parallel semi-permeable silicone membranes (Fig. 1). The liquid PFC flows in each module between the two membranes (PFC-channel) that are externally lapped by gas. Unidirectional PFC flow is obtained with 2 one-way passive valves placed upstream (PV_{IN}) and downstream (PV_{OUT}) the device. The gas-side inlet is connected to a line of compressed oxygenating gas, while the outlet is connected to the atmosphere through an active Solenoid Valve (SV). During the inspiration phase of the respiratory cycle the PFC is actively pumped (pumping phase): SV is close and gas fills and pressurizes the gas side causing tidal volume (TV) ejection. The gas pumping pressure is set by the user via a pressure regulator to adjust the desired TV. During the expiration phase, SV opens to scavenge gas into the atmosphere; therefore, PFC flows into the device due to hydrostatic preload (filling phase). Gas flow is maintained during the filling phase to improve

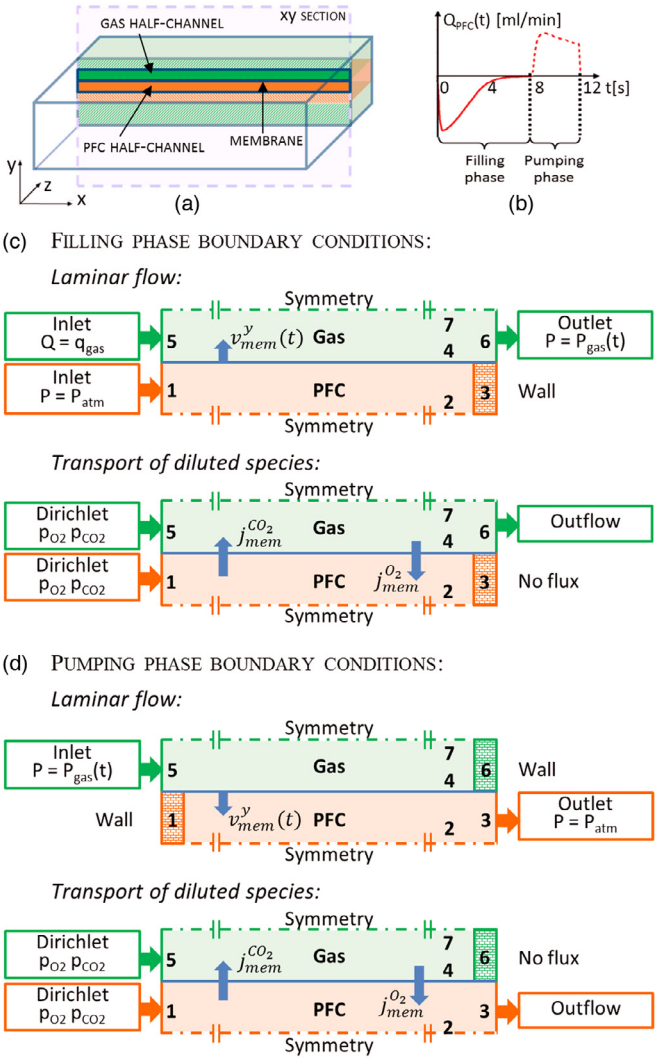

Fig. 2. 2D computational model domain and boundary conditions: (a) geometry of the 2D longitudinal central section: the gas and PFC half-channels used as computational domain are highlighted in the figure; (b) PFC flow rate during the respiratory cycle (solid line = filling phase, dashed line = pumping phase); (c–d) boundary conditions applied at the boundaries during the filling (c) and the pumping (d) phases, for the *laminar flow* and *transport of diluted species modules*.

CO_2 removal from PFC. The PFC flow rate and airway pressure are real-time monitored during the respiratory cycle by an ad hoc implemented control software [22] in order to measure the TV and avoid barotrauma.

The gas exchange occurring in this device strongly depends on the constructive parameters (e.g. shape and dimensions of the silicone membranes, number of modules, etc.). The optimization of the PFC fluid dynamics and gas transfer into each functional module was performed adopting the computational approach described in the following.

2.1. Computational model

In order to reduce the computational cost and simplify the model, the three-dimensional geometry of the oxygenating device was simplified and simulated with a two-dimensional computational model representing one longitudinal section of one functional module (Fig. 2a). To avoid any possible shortcomings introduced by this approximation that neglects flow variations with the depth of the device, a semi-empirical model was implemented, in which an experimental coefficient ξ was introduced. This multiplicative coefficient

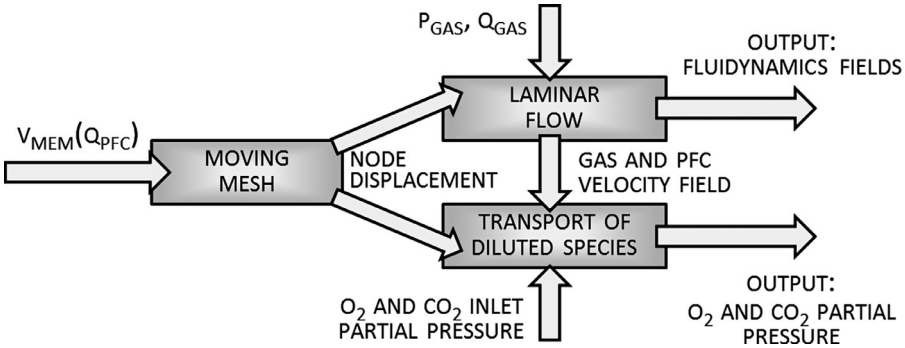

Fig. 3. Flow chart of input and output data between the physics modules used in the computational model.

was calibrated by comparing the model outcomes with experimental data obtained during TLV trials (see Section 2.2 for details).

The model was developed in Comsol Multiphysics 4.3b (Comsol Inc, Burlington, MA, USA). The symmetry permitted to model half functional module, consisting in two adjacent rectangular domains (length: 180–300 mm, gas half-channel thickness: 0.15 mm, PFC half-channel thickness: 0.1 mm) separated by a boundary representing the membrane.

The model contemporaneously analyses three physical aspects: the motion of the membrane, the fluid dynamics of both gas and PFC flowing through the channels, and the O_2 and CO_2 exchange between the two compartments. These three phenomena are implemented using three different physics modules in Comsol Multiphysics: *moving mesh*, *laminar flow* and *transport of diluted species*. The implementation details of the three physics are described in the following and the flow chart of the input and output data between these modules is schematized in Fig. 3.

To simulate the filling and emptying of the PFC channels during each ventilation cycle, the membrane translates in the y direction (Fig. 2a) with a set time-dependent velocity derived from the experimental PFC flow rate curve $Q_{PFC}(t)$ (Fig. 2b):

$$v^{y}_{mem}(t) = -Q_{PFC}(t)/(2 \cdot N \cdot W \cdot L)\ [\mathrm{m/s}] \tag{1}$$

where N is the number of modules, W = 95 mm the PFC chamber width and L the PFC chamber length [mm].

Membrane motion induces the deformation of the domain, implemented in Comsol *moving mesh* module and studied with the numerical approach described by the Arbitrary Lagrange Eulerian (ALE) formulation [23].

Fluid flow in the computational domain was calculated solving Navier–Stokes equations with Comsol *Laminar Flow module*. Unsteady laminar flow conditions were simulated (Reynolds number Re < 30 in the PFC domain and Re < 300 in the gas domain). The fluid in the PFC compartment (Fluorinert™ FC-770, 3 M, St. Paul, MN, USA) was set as Newtonian and incompressible ($\mu = 1.16 \cdot 10^{-3}$ Pa·s, $\rho = 1762$ kg/m^3). The oxygenating gas mixture (O_2 concentration ranging within 70% to 100%) was considered as Newtonian ($\mu = 2.05 \cdot 10^{-5}$ Pa·s) and compressible, to account for density variations induced by pressure changes in the gas domain. The ideal gas law was used to correlate density to gas pressure.

The boundary conditions used to simulate the filling and pumping phases during the ventilation cycle are resumed in Fig. 2 (c and d). Closed passive valves were simulated with a no-slip wall condition applied on *Boundary (B) 3* during the filling phase (PV_{OUT} closed) or *B 1* during the pumping phase (PV_{IN} closed). Atmospheric pressure condition was applied at the PFC inlet (*B 1*) during the filling phase and at the PFC outlet (*B 3*) during the pumping phase.

Also for the gas domain, different boundary conditions were used to simulate the two phases of the ventilation cycle. During the filling phase (Fig. 2c), a laminar gas inflow was applied at *B 5*, setting the flow rate (q_{gas}) equal to the total gas flow rate (Q_{gas}) divided by the number of the gas semi-channels. A time-dependent pressure condition was applied at the gas outlet (*B 6*) to model the pressure decreasing from the gas pumping pressure (P_{gas}) to the atmospheric pressure (P_{atm}), occurring when the SV opens at the beginning of the filling phase. During the pumping phase (Fig. 2d), a no-slip wall condition was used to simulate the closed solenoid valve (SV) at the gas outlet (*B 6*). A time-dependent pressure condition was applied at the gas inlet (*B 5*), to pressurize the gas chamber from P_{atm} to the desired P_{gas}. Symmetry conditions were set at *B 2* and *B 7*.

Oxygen and CO_2 transport in the PFC and gas domains was modeled considering diffusion and convection mass transport mechanisms using Comsol *transport of diluted species module* to solve mass balance equations:

$$\frac{\partial c}{\partial t} = D\nabla^2 c - \mathbf{u} \cdot \nabla c \quad in\ the\ PFC - domain \tag{2}$$

$$\frac{\partial c}{\partial t} = D\nabla^2 c - \nabla \cdot (c\mathbf{u}) \quad in\ the\ Gas - domain \tag{3}$$

where c [mol/m^3] is the concentration of the gas species (i.e. O_2 or CO_2), $\boldsymbol{u}$ [m/s] is the fluid velocity field calculated in the *laminar flow modules*, and D is the diffusion coefficient in the gas ($D_{O2} = 2.32 \cdot 10^{-5}$ m^2/s [24], $D_{CO2} = 1.56 \cdot 10^{-5}$ m^2/s [25]) and in the PFC ($D_{O2} = 5.81 \cdot 10^{-9}$ m^2/s [4], $D_{CO2} = 1.05 \cdot 10^{-9}$ m^2/s [4]).

Dirichlet boundary conditions were applied at the PFC and gas inlets to set CO_2 and O_2 concentrations.

Gas concentrations c in the PFC were calculated with Henry's law ($c = \alpha \cdot p$, where p is the gas partial pressure and α is the gas solubility coefficient in the PFC at 37 °C: $\alpha CO_2 = 0.767 \cdot 10^{-3}$ (mol/m^3)/Pa, $\alpha O_2 = 0.2 \cdot 10^{-3}$ (mol/m^3)/Pa) [26]). CO_2 concentration at gas inlet was always set equal to zero, while O_2 concentration was calculated with Dalton's law knowing the O_2 molar fraction (FiO_2) in the gas mixture.

A no flux condition was applied at the PFC and gas outlets when the outlet valves are closed (i.e. *B 3* during the filling phase or *B 6* during the pumping phase, Fig. 2 (c and d)). Vice versa when the outlet valves are open, an outflow condition was set at the domain outlets (i.e. *B 6* during the filling phase or *B 3* during the pumping phase, Fig. 2 (c and d)). Symmetry conditions were set at the boundaries representing the centre of the two domains (i.e. *B 2* and *B 7*).

The diffusive mass flux through the silicone membrane is defined as:

$$j_{diff}(x,t) = -\mathbf{n} \cdot (-D\nabla c) = \begin{cases} \xi \cdot P_{mem} \cdot (c_{gas}(x,t)RT - c_{PFC}(x,t)/\alpha) & PFC\ \ side \\ \xi \cdot P_{mem} \cdot (c_{PFC}(x,t)/\alpha - c_{gas}(x,t)RT) & Gas\ \ side \end{cases} \tag{4}$$

where: P_{mem} is the membrane permeance to the gas species ($P_{mem,O2} = 1.12 \cdot 10^{-9}$ mol/(s·Pa·m^2), $P_{mem,CO2} = 6.11 \cdot 10^{-9}$ mol/

Table 1
Experimental conditions for the gas exchange in vitro tests and computational model outcomes obtained with the calibrated coefficient ξ.

I:E []	RR [breaths/min]	TV [ml]	$pCO_{2\ PFC,\ IN}$ [mmHg]	$pCO_{2\ PFC,\ OUT\ EXPERIMENT}$ [mmHg]	$pCO_{2\ PFC,\ OUT\ MODEL}$ [mmHg]	ξ_{CO2} []	$pO_{2\ PFC,\ IN}$ [mmHg]	$pO_{2\ PFC,\ OUT\ EXPERIMENT}$ [mmHg]	$pO_{2\ PFC,\ OUT\ MODEL}$ [mmHg]	ξ_{O2} []
1:2	4	15	22.5 ± 0.5	6.9 ± 0.1	6.9	0.24	598 ± 4	752 ± 11	752	0.49
1:2	5	15	22.3 ± 2.2	7.4 ± 0.4	7.4	0.31	592 ± 4	755 ± 18	755	0.70
1:2	6	15	21.3 ± 0.6	7.2 ± 0.3	7.2	0.35	610 ± 9	750 ± 14	750	0.70
1:2	7	15	21.8 ± 0.7	8.3 ± 0.3	8.5	0.35	584 ± 10	740 ± 13	741	0.70
1:1	5	15	22.1 ± 1.1	7.4 ± 0.2	7.4	0.29	614 ± 4	747 ± 18	749	0.50
1:3	5	15	21.2 ± 1.1	6.5 ± 0.4	6.5	0.30	613 ± 14	751 ± 16	748	0.54
1:2	5	35	21.2 ± 0.1	8.8 ± 0.1	8.7	0.61	590 ± 3	751 ± 17	743	1.00
1:2	5	30	22.2 ± 0.2	7.6 ± 0.2	7.6	0.58	608 ± 2	763 ± 12	752	1.00
1:2	5	25	22.6 ± 1.6	8.4 ± 0.5	8.4	0.45	597 ± 7	777 ± 19	759	1.00
1:2	5	22	20.6 ± 0.6	6.5 ± 0.3	6.5	0.44	595 ± 9	755 ± 28	754	0.90
1:2	5	8	21.9 ± 0.4	4.4 ± 0.2	4.4	0.23	597 ± 7	756 ± 24	754	0.43
1:2	5	5	21.1 ± 0.4	7.2 ± 0.5	7.7	0.12	620 ± 9	764 ± 10	761	0.40

Experimental O_2 and CO_2 partial pressure are reported as mean ± standard deviation.

$(s \cdot Pa \cdot m^2)$); c_{gas} and c_{PFC} are the species concentrations at gas and PFC sides of the membrane, respectively [mol/m^3]; R is the universal gas constant (8.314 J/(K·mol)); T is the temperature of the gas (25 °C); α is the gas species solubility in the PFC [$(mol/m^3)/Pa$]; ξ is a multiplicative coefficient calibrated on the experimental outcomes.

Mesh sensitivity analysis led to the discretization of the computational domain with a quadrilateral structured mesh composed by a number of elements ranging within 18,000 to 30,000 depending on the specific geometry analyzed.

For each study case, several respiratory cycles were computed to obtain correct preconditioning of the species concentration in the domains.

2.2. Model calibration and validation

While implementing the model, gas exchange in vitro tests were performed with the aim to calibrate the coefficient ξ to be introduced in Eq. (4). Once the coefficient ξ was properly chosen for both O_2 and CO_2 (i.e. ξ_{O2} and ξ_{CO2} respectively), the reliability of the calibrated model was checked by comparing the model outcomes to further experimental data.

In vitro tests were performed using an ad hoc developed preliminary prototype, named Pro-Li-Ve-22 (N = 22, PFC channel thickness = 0.2 mm, W = 95 mm, L = 180 mm). This device was connected to a test bench (model lung, ML) reproducing neonatal lung impedance and gas exchange [27]. During the experimental trials, the ML was set to reproduce the estimated impedance of a neonatal physiological lung during TLV (inspiratory resistance = 800 $cmH_2O \cdot s/l$, expiratory resistance = 720 $cmH_2O \cdot s/l$, pulmonary compliance = 1 ml/cmH_2O) [27]. In order to test the Pro-Li-Ve gas exchange performance, the PFC at the device inlet had to be conditioned at the O_2 and CO_2 partial pressure values measured during in vivo animal trials in the expired PFC (i.e. $pCO_{2\ PFC,\ IN}$ = 22 ± 3 mmHg, $pO_{2\ PFC,\ IN}$ = 610 ± 30 mmHg, at FiO_2 = 100%) [9]. An oxygenator (Quadrox D, Maquet Cardiopulmonary AG, Hirrlingen, Germany) was used as de-oxygenator to pursue this purpose. During these tests the Pro-Li-Ve was supplied with pure oxygen (FiO_2 = 100%).

Under each test condition, 3 PFC samples were withdrawn at Pro-Li-Ve inlet and outlet and immediately analyzed (ABL725L, Radiometer, Copenhagen, Denmark), to measure CO_2 and O_2 partial pressure. The in vitro tests were performed by varying the ventilation parameters (i.e. TV, Inspiration to Expiration ratio I:E, and Respiratory Rate RR) (Table 1). For each test condition, simulations were performed setting boundary conditions (i.e. $pO_{2\ PFC,\ IN}$, $pCO_{2\ PFC,\ IN}$, $Q_{PFC}(t)$, P_{gas}, Q_{gas}, FiO_2) equal to those acquired during the experiments.

The coefficients ξ_{O2} and ξ_{CO2} were individually calibrated to optimize the matching between the computational results and the experimental data, for each study case (Table 1). The model was considered calibrated when both oxygen and carbon dioxide partial pressures in the PFC at the device outlet calculated with the model were in the range (mean values ± the standard deviation) measured during the experiments (Table 1).

Based on the outcomes of these simulations, analytical relations were found between the coefficients ξ_{O2} and ξ_{CO2} and the mean PFC flow rate (see Results section). Once implemented in the model, these relations permit setting the proper values for ξ_{O2} and ξ_{CO2} even when no experimental data are available. The reliability of this approach was proved by comparing the model outcomes to further experimental data acquired during preliminary in vivo trials performed on juvenile New Zealand rabbits with the preliminary prototype Pro-Li-Ve-22 [19].

Computational simulations were performed setting the boundary conditions to replicate 11 ventilation scenarios, recorded during in vivo trials (Table 2). For each simulation, the model outcomes were compared to these experimental data in terms of gas partial pressure variations in the PFC flowing through the Pro-Li-Ve-22 ($\Delta pCO_{2\ PFC}$ = $pCO_{2\ PFC,\ IN}$ - $pCO_{2\ PFC,\ OUT}$, $\Delta pO_{2\ PFC}$ = $pO_{2\ PFC,\ OUT}$ - $pO_{2\ PFC,\ IN}$), to validate the model.

2.3. Gas transfer optimization in the Pro-Li-Ve

After calibration and validation, the computational model was used to design the optimized Pro-Li-Ve configuration, able to achieve the desired gas partial pressure in the pumped PFC (i.e. $pCO_{2\ PFC,\ OUT}$ = 6.0 ± 0.6 mmHg, $pO_{2\ PFC,\ OUT}$ = 678 ± 32 mmHg) [9] when performing TLV with a ventilation setting suitable for very preterm neonates (i.e. TV = 10, 20, 30 ml, RR = 4, 5, 6 breaths/min, I:E = 1:1, 1:2, 1:3) [6].

The optimized configuration was chosen varying the number of modules (N = 30, 40, 50) and PFC-channel length (L = 180, 220, 260, 300 mm). The optimization study was performed by evaluating the pCO_2 obtained in the pumped PFC (i.e. $pCO_{2\ PFC,\ OUT}$) with the ventilation parameters set at the most onerous condition for CO_2 removal in the Pro-Li-Ve (i.e. TV = 30 ml, RR = 6 breaths/min, I:E = 1:1).

After the optimized configuration was chosen, simulations were run to study the effect on $pO_{2\ PFC,\ OUT}$ and $pCO_{2\ PFC,\ OUT}$ exerted by the variation of the ventilation parameters.

For all simulations, gas partial pressures at the PFC inlet were set to the typical PFC expiration conditions reported in the literature for TLV in vivo trials ($pCO_{2\ PFC,\ IN}$ = 22 mmHg and $pO_{2\ PFC,\ IN}$ = 610 mmHg [9]).

TABLE 2
Experimental in vivo conditions and computational outcomes used for model validation.

I:E []	RR [breaths/min]	TV [ml]	FiO_2 [%]	$pCO_{2\ PFC,\ IN}$ [mmHg]	$pCO_{2\ PFC,\ OUT\ EXPERIMENT}$ [mmHg]	$pCO_{2\ PFC,\ OUT\ MODEL}$ [mmHg]	$\varepsilon\%\Delta pCO_{2\ PFC}$ [%]	$pO_{2\ PFC,\ IN}$ [mmHg]	$pO_{2\ PFC,\ OUT\ EXPERIMENT}$ [mmHg]	$pO_{2\ PFC,\ OUT\ MODEL}$ [mmHg]	$\varepsilon\%\Delta pO_{2\ PFC}$ [%]
1:2	6	23.5	100	38.4	14.1	14.8	−2.9	598	756	754	−1.4
1:2	6	23.1	100	35.7	13.7	13.7	0.1	581	733	750	10.9
1:2	5	23.9	100	38.6	15.4	14.5	4.0	539	756	749	−3.2
1:2	6	25.2	100	38.6	14.6	15.2	−2.4	592	732	748	11.8
1:2	7	23.4	72	35.6	14.3	14.0	1.5	409	537	533	−2.8
1:2	7	23.5	72	34.2	12.4	13.5	−4.9	379	521	526	3.2
1:2	6	30.2	100	42.8	17.7	16.2	5.9	615	742	752	7.5
1:2	6	30.2	100	42.5	16.3	16.2	0.6	601	730	748	13.6
1:3	6	25.4	100	48.4	16.5	17.0	−1.6	584	754	752	−1.4
1:2	6.5	29.0	100	37.2	15.9	15.0	4.2	629	748	756	7.1
1:1	6.5	29.5	100	39.8	17.8	17.8	0.2	573	742	742	0.2

The percentage errors are defined as:
$\varepsilon\%\Delta pCO_{2\ PFC} = [(pCO_{2\ PFC,IN}\text{-}pCO_{2\ PFC,OUT\text{-}MODEL})\text{-}(pCO_{2\ PFC,IN}\text{-}pCO_{2\ PFC,OUT\text{-}EXPERIMENT})]/(pCO_{2\ PFC,IN}\text{-}pCO_{2\ PFC,OUT\text{-}EXPERIMENT})$;
$\varepsilon\%\Delta pO_{2\ PFC} = [(pO_{2\ PFC,OUT\text{-}MODEL}\text{-}pO_{2\ PFC,IN})\text{-}(pO_{2\ PFC,OUT\text{-}EXPERIMENT}\text{-}pO_{2PFC,IN})]/(pO_{2\ PFC,OUT\text{-}EXPERIMENT}\text{-}pO_{2\ PFC,IN})$.

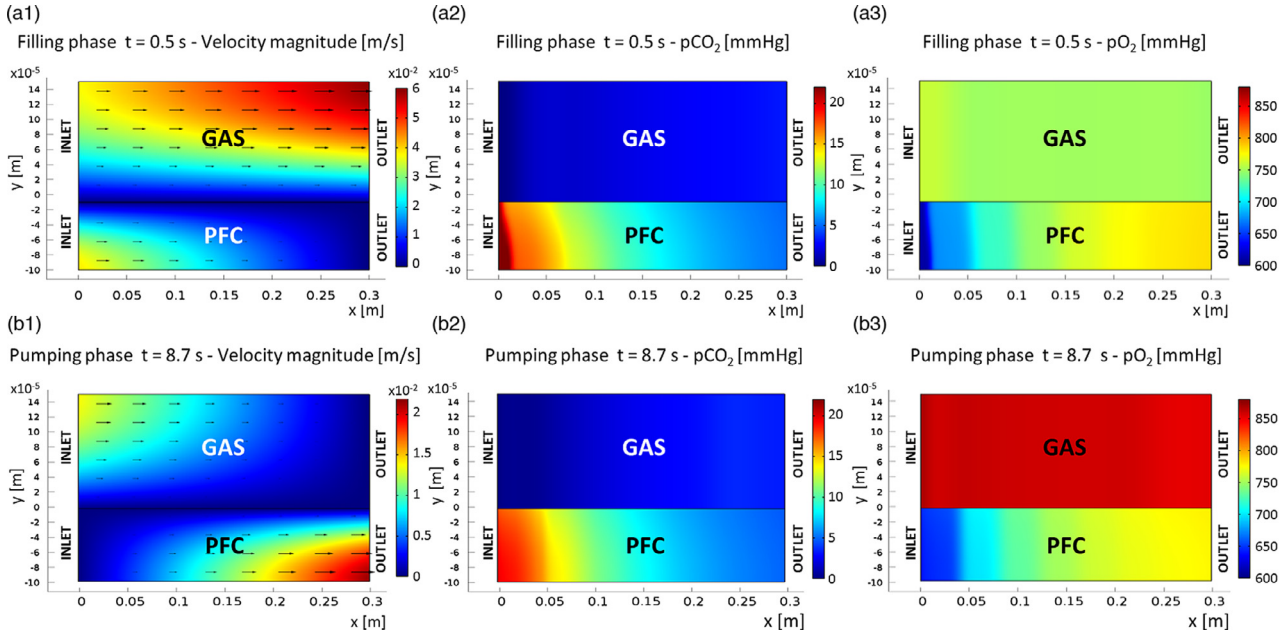

Fig. 4. Velocity field (1) and CO_2 (2) and O_2 (3) partial pressure: (a) at the velocity-peak during the filling phase (t = 0.5 s); (b) at the velocity-peak during the pumping phase (t = 8.7 s). The *x* and *y* axes in the plots are re-scaled in order to permit proper visualization of the results. Simulation parameters: TV = 30 ml, P_{gas} = 110 mmHg, Q_{gas} = 1.8 l/min, RR = 5 breaths/min, I:E = 1:2, $pCO_{2\ PFC,IN}$ = 22 mmHg, $pO_{2\ PFC,IN}$ = 610 mmHg, N = 40, L = 300 mm.

3. Results

3.1. Computational model outcomes

The colour-maps of velocity and CO_2 and O_2 partial pressure at two different instants of the ventilation cycle (i.e. $t = 0.5$ s during the filling phase and $t = 8.7$ s during the pumping phase) are shown in Fig. 4. During the filling phase (Fig. 4a), the translation of the membrane toward the positive direction of the *y*-axis causes PFC to flow into the computational domain (Fig. 4a1) with a typical laminar flow profile. Thus, the expired PFC, loaded with CO_2 and poor in O_2, fills the inlet of the PFC channel. The gas pressure decrease at the beginning of the filling phase causes the outlet of the oxygenating mixture from the computational domain; as a consequence, the pCO_2 (Fig. 4a2) and pO_2 (Fig. 4a3) in the gas domain undergo a decrease. A continuous gas flow is maintained throughout the filling phase in the gas channel (Fig. 4a1), in order to keep low pCO_2 values, despite the CO_2 diffusion into the gas domain.

During the pumping phase (Fig. 4b), PFC flows out from the computational domain as a result of the membrane translation toward the *y*-axis negative direction, inducing a reduction in the PFC domain area (Fig. 4b1); laminar flow is observed in the PFC domain. The oxygenating gas mixture flowing into the gas domain pressurizes it at the beginning of the pumping phase, inducing an increase in the pCO_2 (Fig. 4b2) and pO_2 (Fig. 4b3) values in the gas domain. Diffusive gas transfer occurs between the gas and PFC domains, thus, the pumped PFC at the domain outlet is oxygenated and poor in CO_2.

3.2. Results of model calibration and validation

In vitro gas exchange obtained with the preliminary Pro-Li-Ve-22 at different ventilation conditions are reported in Table 1. The values for ξ_{CO2} and ξ_{O2} reported are the calibrated coefficients that permit to achieve the best matching between experimental and computational outcomes.

A linear correlation between ξ_{CO2} and the mean PFC flow rate through a single module (Q_{PFC}) fits with an adequate accuracy the data points ($R^2 = 0.97$) (Fig. 5a). As regards the oxygen exchange model, a piecewise linear correlation between ξ_{O2} and Q_{PFC} best fits the data points ($R^2 = 0.92$) (Fig. 5b). The correlation equations, resulting from the calibrating procedure, allow the identification of a single value of both ξ_{O2} and ξ_{CO2} for each Q_{PFC} that can be set as an input

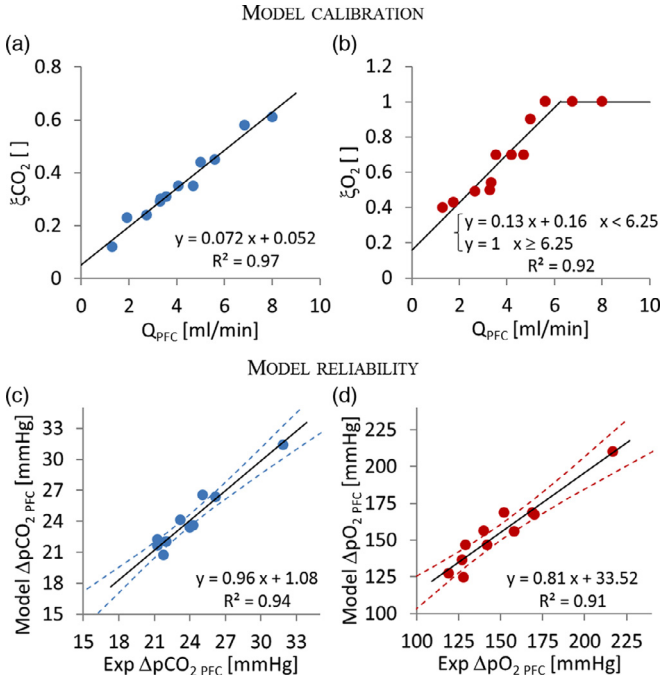

Fig. 5. Upper - model calibration: linear correlation between ξ_{CO2} (a) and ξ_{O2} (b) and the mean PFC flow rate through each module (Q_{PFC}[ml/min] = TV[ml]/N·RR[breaths/min]). Bottom - model reliability: comparisons between the model predicted and in vivo experimental measured $\Delta pCO_{2\,PFC}$ (c) and $\Delta pO_{2\,PFC}$ (d). The solid lines represent the linear regression lines, with the 95% confidence intervals (dashed lines).

of the model. These equations (Fig. 5 (a and b)) were implemented in the model to predict ξ_{O2} and ξ_{CO2} when running the following simulations.

The comparison between the PFC data recorded during experimental in vivo tests [19] and the computational $\Delta pCO_{2\,PFC}$ and $\Delta pO_{2\,PFC}$ outcomes is shown in Fig. 5 (c and d). Regression lines slopes (mCO_2 and mO_2) approach the unity, proving the goodness of the model predictions (95% confidence intervals of regression lines slope: mCO_2 = [0.77, 1.14] and mO_2 = [0.62, 1.01]). Overall, the model predicts experimental gas exchange results with a good accuracy (mean percentage error: $\varepsilon_{\%}\Delta pCO_{2\,PFC}$ = 2.6, $\varepsilon_{\%}\Delta pO_{2\,PFC}$ = 5.7, Table 2).

3.3. Results of the gas transfer optimization in the Pro-Li-Ve

CO_2 partial pressure in the pumped PFC is presented in Fig. 6a as a function of the different geometrical parameters (N, L) simulated with the computational model. The goal $pCO_{2\,PFC,\,OUT}$ (6.0 ± 0.6 mmHg) would be obtainable with a prototype comprising 40 modules at least 300 mm in length, or 50 modules at least 260 mm in length. The first option (N = 40, L = 300 mm) was chosen for the optimized device (named Pro-Li-Ve-40). Indeed, compared to the second option (N = 50, L = 260 mm), a smaller membrane surface area (2.28 m^2 vs. 2.47 m^2) and a smaller priming volume (228 ml vs. 247 ml) are required, which means lower cost both for the production of the ventilator and for the PFC necessary for the TLV treatments.

The O_2 and CO_2 partial pressures in the PFC pumped by the Pro-Li-Ve-40 as a function of ventilation parameters are shown in Fig. 6 (b–h). PFC oxygen partial pressure is higher than the target values (678 ± 32 mmHg) for all the considered conditions with FiO_2 = 100%, which means a high oxygenating efficiency of the device. However, the target $pO_{2\,PFC,\,OUT}$ can be easily obtained by reducing the oxygen concentration in the gas mixture (e.g. FiO_2 = 80–90%, Fig. 6b). O_2 partial pressure in the PFC shows a tendency to increase with the increasing of TV or I:E and the decreasing of RR (Fig. 6 (c, d and e)).

The CO_2 partial pressure in the pumped PFC increases when TV, RR or I:E ratio increase (Fig. 6 (f, h and g). However, $pCO_{2\,PFC,\,OUT}$ is lower than the maximum target values (6.0 ± 0.6 mmHg) for all the considered cases, suggesting that an adequate CO_2 removal efficiency is maintained.

4. Discussions

The expediency of a computational approach to study gas transfer phenomena in the Pro-Li-Ve arises from the necessity to predict and quantify the effects of fluid dynamics and geometric parameters on the device performance prior to construct the prototypes. Therefore, a computational model able to accurately reproduce gas transfer in the ventilator is a time-saving tool for the design of the optimal Pro-Li-Ve, able to comply with the technical specifications.

The choice of Comsol Myltiphysics as a solver is due to the features of this software that allow the modeling of coupled fluid flow and mass transport phenomena.

Some simplifying hypotheses were assumed to reduce the computational cost while maintaining model accuracy. The modularity of the device combined with the assumption of equal distribution of the TV in each PFC-channel, allowed considering only one functional module of the device. Moreover, the symmetry of the problem permitted simulating only half PFC-chamber and the adjacent half gas-channel. The use of a 2D model simulating only one section of the module implies that the real domain is represented as a perfect parallelepiped, neglecting the variation of the channel thickness at the lateral borders, occurring in the real device.

In the real device, PFC flow is induced by membrane deformation as a result of pressure variations in the gas channel. This mechanism would be reproducible in silico with a fluid-structure interaction approach, but requiring about one order of magnitude higher computational costs, which have been avoided by simulating the membrane motion with a simple translation.

Possible uncertainties related to materials properties (e.g. membrane gas permeance), construction tolerances and PFC not perfectly homogeneous distribution in the Pro-Li-Ve prototypes are considered in this semi-empirical model by the multiplicative coefficients ξ_{O2} and ξ_{CO2}, introduced in Eq. 4. These coefficients were calibrated on the experimental results obtained from the in vitro TLV tests. Both coefficients ξ_{O2} and ξ_{CO2} were supposed correlated to the mean PFC flow rate in each PFC channel (Q_{PFC}) (i.e. correlation coefficients: $corr(\xi_{O2,}\, Q_{PFC}) = 0.94$, $corr(\xi_{CO2,}\, Q_{PFC}) = 0.99$). Both ξ_{O2} and ξ_{CO2} in-crease, approaching to 1, with the increment of Q_{PFC}. This could be ex-plained by observing that the PFC-channels are more recruited with a high Q_{PFC}, and possible inaccuracies in the real manufactured prototype are reduced, getting closer to the ideal situation simulated.

Eventually, the model reliability was proved by comparing computational results with experimental outcomes: 11 different ventilation situations, from preliminary in vivo trials, were considered. The model proved to calculate gas exchange in the Pro-Li-Ve with a good accuracy, thus it was used to evaluate Pro-Li-Ve gas exchange performance as a function of its geometry, allowing finding the opti-mal configuration. Simulations proved that Pro-Li-Ve-40 (N = 40, L = 300 mm, Exchange surface area = 2.28 m^2) allows obtaining the desired gas exchanges for very preterm neonatal TLV applications.

Ventilation parameters were varied in the range reported in the literature [5,6] predicting good performance of the device in the entire investigated range. The model permitted to highlight the gas exchange dependence on the different ventilation parameters: PFC residence time in the device, gas partial pressure difference between the two sides of the membrane, and PFC flow rate Q_{PFC}, affecting ξ_{O2} and ξ_{CO2} coefficients. An increase in TV leads to an increase in ξ_{O2} and ξ_{CO2} (i.e. higher gas exchange), but to a shortening of the PFC

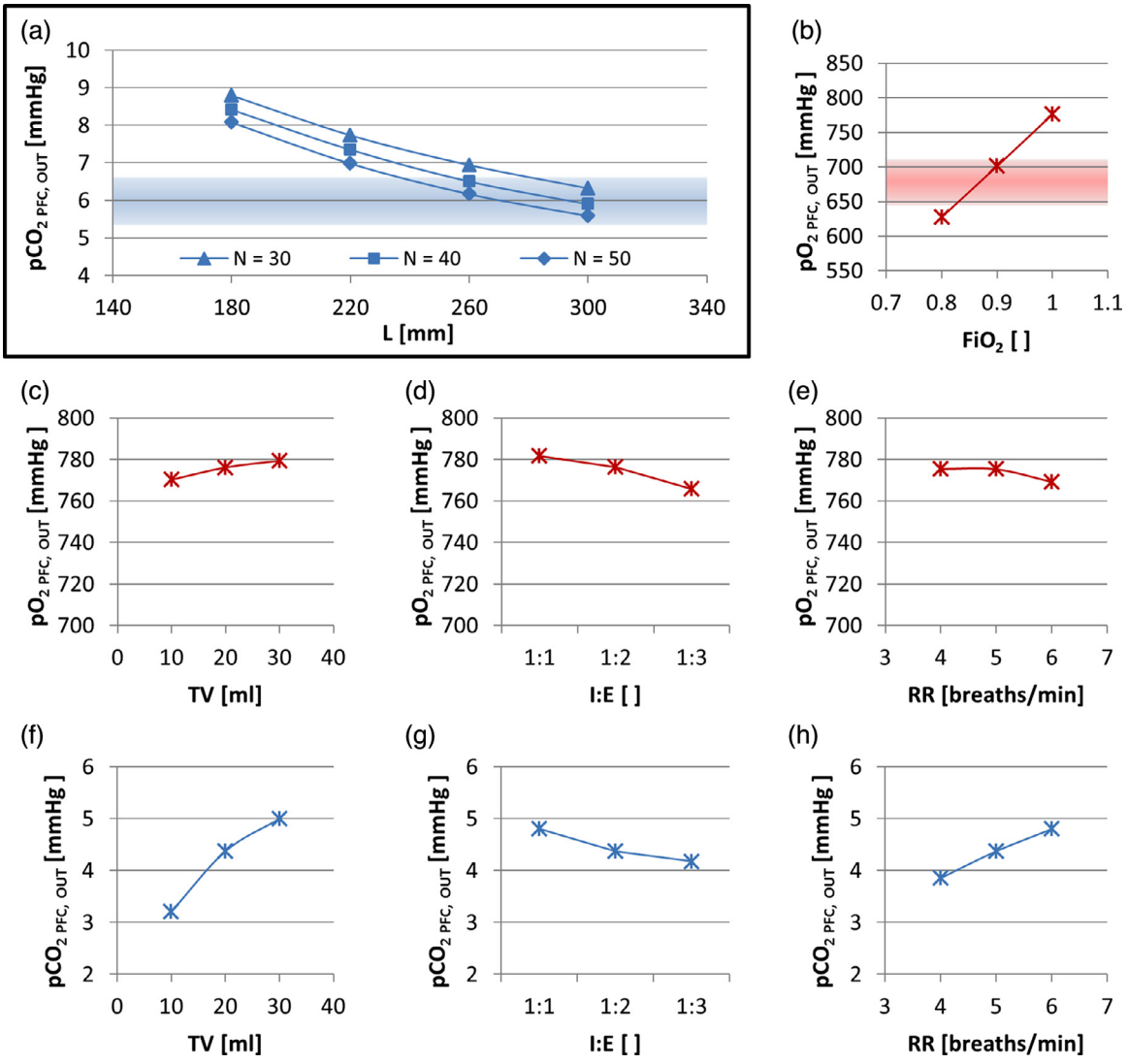

Fig. 6. (a) pCO_2 in the pumped PFC as a function of the Pro-Li-Ve parameters (i.e. number of modules N = 30, 40, 50; length L = 180, 220, 260, 300 mm) obtained with the ventilation setting: TV = 30 ml, RR = 6 breaths/min, I:E = 1:1. The highlighted band corresponds to the maximum pCO_2 value acceptable in the pumped PFC (i.e. $pCO_{2\,PFC,\,OUT}$ = 6.0 ± 0.6 mmHg). (b–h) pO_2 and pCO_2 obtained from the simulations of the optimized Pro-Li-Ve (N = 40, L = 300 mm) as a function of the ventilation parameters: (b) pO_2 vs. FiO_2, the highlighted band corresponds to the desired pO_2; (c) pO_2 vs. TV; (d) pO_2 vs. I:E; (e) pO_2 vs. RR; (f) pCO_2 vs. TV; (g) pCO_2 vs. I:E; (h) pCO_2 vs. RR. If not differently reported, the ventilation setting is: TV = 20 ml, RR = 5 breaths/min, I:E = 1:2, FiO_2 = 100%, $pO_{2\,PFC,\,IN}$ = 610 mmHg, $pCO_{2\,PFC,\,IN}$ = 22 mmHg.

residence time (i.e. lower gas exchange). The sum of these two opposite effects affects the device exchange performance at different TV. In particular, two opposite trends for O_2 and CO_2 are found from computational simulations (Fig. 6 (c and f)): a higher TV results in a higher $\Delta pO_{2\,PFC}$ but in a lower $\Delta pCO_{2\,PFC}$. This can be explained observing that ξ_{O2} variation is higher than the variation of ξ_{CO2}, when varying the TV from 10 ml to 30 ml (i.e. $\Delta\xi_{O2} = 0.34$ and $\Delta\xi_{CO2} = 0.18$). As regards the respiratory rate, the higher the RR the lower the gas vs. PFC flow rate ratio and the PFC residence time; both effects reduce gas exchange efficiency. Otherwise, an increase in RR causes an increase in ξ coefficients. The overall effect is a tendency to gas exchanges decrease both for O_2 and CO_2 (Fig. 6 (e and h)). Inspiration to expiration ratio exerts an opposite effect on O_2 and CO_2 transfer. The CO_2 exchange is favoured at lower I:E (Fig. 6g), since with a longer expiration the continuous gas flow throughout the device during the filling phase maximizes the pCO_2 difference between the gas and PFC sides. Vice versa O_2 transfer benefits from higher I:E (Fig. 6d), since with a longer inspiration the gas pressure is maintained high for a longer period (i.e. pumping phase), thus increasing the pO_2 in the gas channel. FiO_2 adjustment in the oxygenating mixture permits obtaining the proper oxygen concentration in the pumped PFC (Fig. 6b), avoiding the risks related to hyperoxia. This issue is particularly crucial when preterm or neonatal patients are concerned, since too high oxygen levels in the patient blood may cause alveolar damage and induce severe chronical injury (e.g. hyperoxia-related retinopathies). Therefore, during TLV the PFC oxygen partial pressure must be properly modulated to obtain the desired blood oxygenation, by varying the O_2 percentage in the gas mixture that flows through the device.

5. Conclusions

This study provided a validated computational model to predict O_2 and CO_2 exchange in an innovative ventilator prototype for TLV, the Pro-Li-Ve. The model permits to quantitatively evaluate the effects on the gas exchange exerted by the ventilation parameters used during TLV in the typical setting for very preterm neonatal applications.

The guidelines provided by the model for the design of the optimal configuration of the Pro-Li-Ve are fundamental to obtain an efficient device capable to guarantee performant gas transfer in a compact and low priming volume circuit. The findings of this study are at the basis

of the construction of the new Pro-Li-Ve prototype that can meet the gas exchange and safety requirements for clinical applications.

Conflict of interest

No conflict of interest to disclose. The authors have no financial and personal relationship that could inappropriately influence their work.

Ethical approval

Not applicable for this study.

Acknowledgments

This work was supported by the Italian Ministry of Education, University and Research (grant FIRB 2008 – Futuro in Ricerca – RBFR081BZQ). The authors thank Dr. Sara Arlati for her contribution to the initial phase of the project.

References

[1] Wu ZL, Taskin ME, Zhang T, Fraser KH, Griffith BP. Computational model-based design of a wearable artificial pump-lung for cardiopulmonary/respiratory support. Artif Organs 2012;36(4):387–99.
[2] Hormes M, Borchardt R, Mager I, Schmitz-Rode T, Behr M, Steinseifer U. A validated CFD model to predict O_2 and CO_2 transfer within hollow fiber membrane oxygenators. Int J Artif Organs 2011;34(3):317–25.
[3] Suresh V, Anderson JC, Grotberg JB, Hirschl RB. A mathematical model of alveolar gas exchange in partial liquid ventilation. J Biomech Eng 2005;127(1):46–59.
[4] Corno C, Fiore GB, Costantino ML. A mathematical model of neonatal tidal liquid ventilation integrating airway mechanics and gas transfer phenomena. IEEE Trans Biomed Eng 2004;51(4):604–11.
[5] Wolfson MR, Shaffer TH. Pulmonary applications of perfluorochemical liquids: ventilation and beyond. Pediatr Respir Rev 2005;6(2):117–27.
[6] Foley DS, Hirschl RB. Liquid ventilation. In: Mac Intyre NR, Branson RD, editors. Mechanical ventilation. W.B. Saunders Company; 2001. p. 433–53.
[7] Bagnoli P, Tredici S, Seetharamaiah R, Brant DO, Hewell LA, Johnson K, et al. Effect of repeated induced airway collapse during total liquid ventilation. ASAIO J 2007;53(5):549–55.
[8] Sekins KM, Nugent L, Mazzoni M, Flanagan C, Neer L, Rozenberg A, Hoffman J. Recent innovations in total liquid ventilation system and component design. Biomed Instrum Technol 1999;33(3):277–84.
[9] Tredici S, Komori E, Funakubo A, Brant DO, Bull JL, Bartlett RH, Hirschl RB. A proto-type of a liquid ventilator using a novel hollow-fiber oxygenator in a rabbit model. Crit Care Med 2004;32(10):2104–9.
[10] Meinhardt JP, Quintel M, Hirschl RB. Development and application of a double-piston configured, total-liquid ventilatory support device. Crit Care Med 2000;28(5):1483–8.
[11] Robert R, Micheau P, Cyr S, Lesur O, Praud JP, Walti H. A prototype of volume-controlled tidal liquid ventilator using independent piston pumps. ASAIO J 2006;52(6):638–45.
[12] Corno C, Fiore GB, Martelli E, Dani C, Costantino ML. Volume controlled apparatus for neonatal tidal liquid ventilation. ASAIO J 2003;49(3):250–8.
[13] Bhutani VK, Shaffer TH. Effect of liquid ventilation on preterm lamb tracheal mechanics. Biol Neonate 1983;44(5):257–63.
[14] Bull JL, Foley DS, Bagnoli P, Tredici S, Brant DO, Hirschl RB. Location of flow limitation in liquid-filled rabbit lungs. ASAIO J 2005;51(6):781–8.
[15] Bagnoli P, Acocella F, Di Giancamillo M, Fumero R, Costantino ML. Finite element analysis of the mechanical behavior of preterm lamb tracheal bifurcation during total liquid ventilation. J Biomech 2013;46(3):462–9.
[16] Costantino ML, Micheau P, Shaffer TH, Tredici S, Wolfson MR. Clinical design func-tions: round table discussions on the bioengineering of liquid ventilators. 6th Internationl Symposium on Perfluorocarbon Application and Liquid Ventilation. ASAIO J 2009;55(3):206–8.
[17] Robert R, Micheau P, Avoine O, Beaudry B, Beaulieu A, Walti H. A regulator for pressure-controlled total-liquid ventilation. IEEE Trans Biomed Eng 2010;57(9):2267–76.
[18] Bagnoli P, Fumero R, Costantino ML. A New Lung-Protective Total Liquid Ventila-tion Device. ASAIO J 2008;54(2):60A.
[19] Bagnoli P, Acocella F, Bonfanti M, Canta A, De Gaetano F, Ghiringhelli M, et al. A new non-volumetric pulsatile ventilator prototype for neonatal Total Liquid Ven-tilation. In: Proceedings of GNB2014, June 25th-27th 2014, B-27; 2014. p. 1–3. Bologna: Pàtron EdISBN: 9788855532754.
[20] Fiore GB, Costantino ML, Fumero R, Montevecchi FM. The pumping oxygenator: design criteria and first in vitro results. Artif Organs 2000;24(10):797–807.
[21] Bird RB, Stewart WE, Lightfoot EN. Diffusivity and the mechanism of mass transport. Transport Phenomena. 2nd ed. John Wiley & Sons; 2007.
[22] Bagnoli P, Bonfanti M, Costantino ML. A new software control with safety feedback on airway pressure for a total liquid ventilation prototype. In: Proceedings of ASAIO 60th Annual Conference; 2014. p. 99. Paper 119ASAIO J.
[23] Donea J, Huerta A, Ponthot JP, Rodríguez–Ferran A. Arbitrary Lagrangian–Eulerian methods. In: Stein E, De Borst R, Hughes TJR, editors. Encyclopedia of Computational Mechanics, vol. 1. John Wiley & Sons; 2004. p. 414–37.
[24] Winn EB. The temperature dependence of the self-diffusion coefficients of argon, neon, nitrogen, oxygen, carbon dioxide, and methane. Phys Rev 1950;80(6):1024–7.
[25] Cussler EL. Diffusion coefficients. Diffusion: Mass transfer in fluid systems. 3rd ed. Cambridge Series in Chemical Engineering; 2009.
[26] Kaisers U, Kelly KP, Busch T. Liquid Ventilation. Br J Anaesth 2003;91(1):143–51.
[27] Bagnoli P, Vismara R, Fiore GB, Costantino ML. A mechanical model lung for hydraulic testing of total liquid ventilation circuits. Int J Artif Organs 2005;28(12):1232–41.